

MANIPULATING TRANSMISSION AND REFLECTION PROPERTIES OF A PHOTONIC CRYSTAL DOPED WITH QUANTUM DOT NANOSTRUCTURES

*G. Solookinejad, M. Panahi, E. A. Sangachin, S. H. Asadpour**

Department of Physics, Marvdasht Branch, Islamic Azad University, Marvdasht, Iran

Received April 29, 2016

The transmission and reflection properties of incident light in a defect dielectric structure is studied theoretically. The defect structure consists of donor and acceptor quantum dot nanostructures embedded in a photonic crystal. It is shown that the transmission and reflection properties of incident light can be controlled by adjusting the corresponding parameters of the system. The role of dipole–dipole interaction is considered as a new parameter in our calculations. It is noted that the features of transmission and reflection curves can be adjusted in the presence of dipole–dipole interaction. It is found that the absorption of weak probe light can be converted to the probe amplification in the presence of dipole–dipole interaction. Moreover, the group velocity of transmitted and reflected probe light is discussed in detail in the absence and presence of dipole–dipole interaction. Our proposed model can be used as a new all-optical devices based on photonic materials doped with nanoparticles.

DOI: 10.7868/S0044451016120051

1. INTRODUCTION

Quantum coherence and interference phenomena have been studied due to their potential applications in quantum information science and the development of all-optical devices in past decades by many research groups [1–13]. In this case, controlling the group velocity of transmitted light from different media in view of its potential application in quantum information processing has been discussed by different groups [14–19]. It has been shown that the group velocity of the probe light can be switched between superluminal and subluminal light propagation by adjusting some controllable parameters of the system. However, there is potential interest in studying the group velocity of transmitted and reflected pulses simultaneously in different structures. For this reason, transmission and reflection properties of incident light in a defect slab medium have been discussed from the standpoint of adjusting the group velocity of transmitted and reflected pulses in [20]. In another study [21], the group velocity of the transmitted and reflected pulses from defect slab via spontaneously generated coherence (SGC) and an incoherent pumping field was discussed. It was noted in

[21] that the group velocity of transmitted and reflected pulses from defect slab can be adjusted by controlling the system parameters. Very recently a new model for controlling the group velocity of the transmitted and reflected light from defect slab via the quantum coherence effect was proposed [22]. It was noted that the relative phases of applied fields can be used as potential parameters for adjusting the time delay of transmitted and reflected light beams. In fact, achieving simultaneous subluminal or superluminal light propagation in the transmitted and reflected pulses is of interest for the use in quantum information technology.

In this paper, we present a new model for studying the properties of transmitted and reflected pulses from defect slab doped with a photonic crystal with acceptor and donor quantum dots. The dipole–dipole interaction (DDI) effect has been studied in many research works. In fact, DDI becomes important when the density of doped quantum dots is high. The behavior of DDI coupling parameters in polaritonic band gap materials doped with dense three-level quantum dot nanostructures has been investigated by Singh by studying absorption properties of weak probe light. It has been found that with increasing the strength of DDI coupling parameters, the absorption coefficient decreases. Therefore, the DDI coupling parameters can be used for manipulating the electromagnetically induced transparency windows [23]. The spontaneous

* E-mail: s.hosein.asadpour@gmail.com

emission cancelation in photonic band gap materials doped with nanoparticles have also discussed by Singh in the presence of the DDI coupling parameter [24]. The refractive index properties of a metallic photonic crystal highly doped with four-level nanoparticles was also presented in [25]. It has been demonstrated that in the presence of electron–photon interaction, two transparency windows are predicted in the dipole approximation. Dipole–dipole interaction in a quantum dot and a metallic nanorod hybrid system has been analyzed by using the density matrix method [26]. It has been found that two transparency states can be switched to one transparency window by adjusting the control field in the presence of the DDI coupling parameter. In another study, the effect of DDI and energy transfer in a nonlinear photonic crystal doped with quantum dots and graphene nanodisks are discussed [27]. Due to the presence of DDI, the excitons in a quantum dot and surface plasmon polaritons in a graphene nanodisk, the nonlinear photonic crystal can be used as a tunable photonic reservoir for quantum dots and used to adjust the energy transfer. It has been found that the power absorption spectrum in the quantum dot has two peaks due to the DDI. Very recently, the optical bistability and multistability of a nonlinear photonic crystal doped with acceptor and donor quantum dots have been reported in [28]. It was found that due to presence of the DDI coupling parameter, the properties of bistability and multistability optical can be adjusted and interesting results can be obtained.

In this study, we discuss the transmission and reflection coefficients of incident light in a medium doped with a nonlinear photonic crystal and two acceptor and donor quantum dots. We consider the effect of DDI on the transmitted and reflected pulses and discuss the group velocity of reflected and transmitted light beams.

2. MODEL AND EQUATIONS

For studying the behavior of transmission and reflection properties of incident light, we consider a defect dielectric medium consisting of a photonic crystal with doped acceptor and donor quantum dot (QD) nanostructures. Some properties of photonic crystals such as the dispersion relation of the Bloch photons can be found in [29]. Each of the QDs has two excited states $|3\rangle$ and $|2\rangle$, and the ground state $|1\rangle$ (Fig. 1a). Further details about this type of structure can be found in [28]. States $|1\rangle$ and $|2\rangle$ are coupled by probe light with a Rabi frequency Ω_p . A coupling field with the amplitude E_c and Rabi frequency Ω_c drives the transition $|2\rangle \rightarrow |3\rangle$.

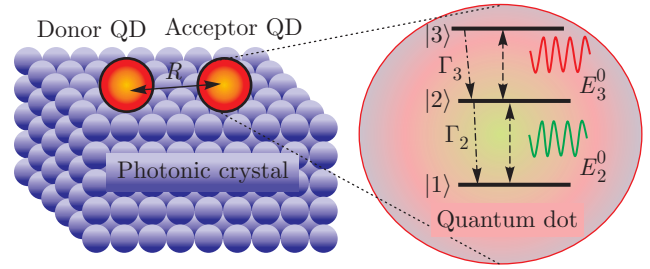


Fig. 1. A configuration of donor and acceptor quantum dots embedded in a photonic crystal. The states of quantum dots are presented by $|1\rangle$, $|2\rangle$ and $|3\rangle$

Moreover, it is assumed that the donor and acceptor QDs can interact with each other via DDI. In the acceptor QD, due to the induced dipole, the polarization can be expressed as $P_a = \mu_{12}\rho_{21} + \mu_{23}\rho_{23}$. The dipole electric field E^a in the donor QD due to the polarization in the acceptor QD is given by $E^a = S_a P_a / (4\pi\epsilon_0)\epsilon_{eff}R^3$, where R is the distance between the acceptor and donor and S_a is called the polarization parameter, which has the value $S_a = 2$ or $S_a = -1$. We have the parameter $\epsilon_{eff} = 3\epsilon_p / (2\epsilon_p + \epsilon_Q)$, where ϵ_Q denotes the dielectric constant of the QDs and ϵ_p is the dielectric constant of the photonic crystal. The expression for the acceptor electric field can be given by

$$E^a = \frac{\hbar}{\mu_{12}D_{21}\rho_{21}} + \frac{\hbar}{\mu_{23}D_{32}\rho_{32}}, \quad (1)$$

$$D_{21} = \frac{3\epsilon_p(\omega_{21})\mu_{12}^2 S_a}{4\pi\epsilon_0\hbar R^3 (2\epsilon_p(\omega_{21}) + \epsilon_Q)}, \quad (2)$$

$$D_{32} = \frac{3\epsilon_p(\omega_{32})\mu_{32}^2 S_a}{4\pi\epsilon_0\hbar R^3 (2\epsilon_p(\omega_{32}) + \epsilon_Q)}. \quad (3)$$

The dipole electric field is related to the density matrix elements ρ_{21} and ρ_{12} and the distance between the acceptor and the donor, which is of the order of a nanometer [29]. The DDI Hamiltonian in the rotating wave approximation can be expressed as

$$H_{DDI} = -(\hbar D_{21}\rho_{21}\sigma_{21}^+ + \hbar D_{32}\rho_{32}\sigma_{32}^+) + \text{H.c.}, \quad (4)$$

where $\sigma_{21}^+ = |2\rangle\langle 1|$, $\sigma_{32}^+ = |3\rangle\langle 2|$ and H.c. denotes Hermitian conjugate terms. The parameters D_{21} and D_{32} are called the DDI coupling parameters. The photonic crystal acts as a reservoir for the donor and acceptor, leading excitons to interact with Bloch photons and decay spontaneously from $|2\rangle$ to $|1\rangle$ and from $|3\rangle$ to $|2\rangle$. By using the density matrix method, the equation of motion can be obtained in the form

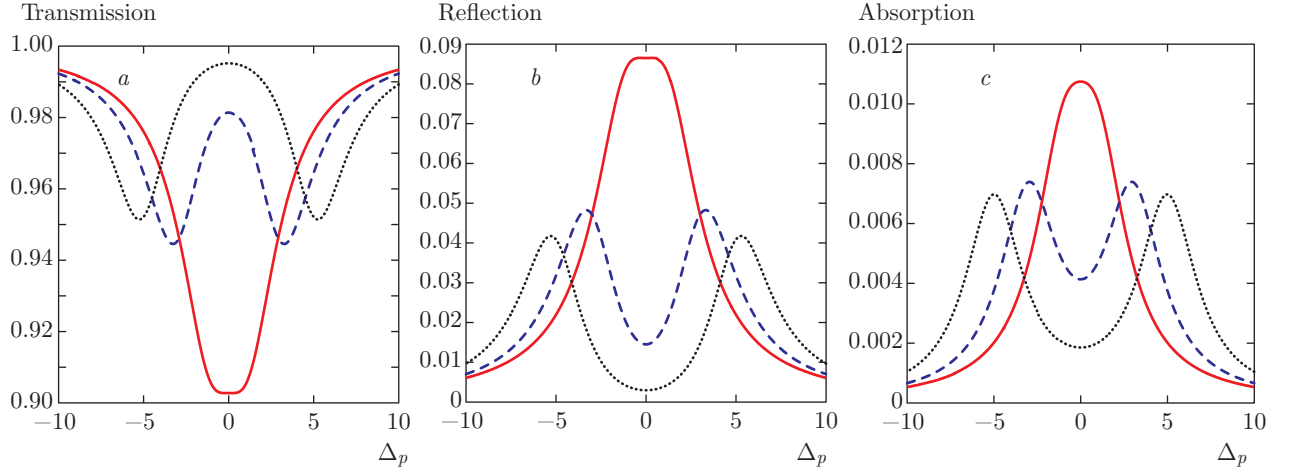


Fig. 2. (a) Transmission, (b) reflection, and (c) absorption properties of incident light versus the probe field detuning for different quantities of the Rabi frequency. The solid lines correspond to $\Omega_c = 2.5$, the dashed lines to $\Omega_c = 5$, and the dotted lines to $\Omega_c = 7.5$. The selected parameters are $m = 100$, $D_{21} = D_{32} = 0$, $\lambda_0 = 1.55 \mu\text{m}$, and $\Delta_c = 0$

$$\begin{aligned}
\frac{\partial \rho_{11}}{\partial t} &= \Gamma_2 \rho_{22} - i(\Omega_p + D_{21} \rho_{21}) \rho_{12} + \\
&\quad + i(\Omega_p + D_{21}^* \rho_{12}) \rho_{21}, \\
\frac{\partial \rho_{33}}{\partial t} &= -\Gamma_3 \rho_{33} - i(\Omega_c + D_{32}^* \rho_{23}) \rho_{32} + \\
&\quad + i(\Omega_c + D_{32} \rho_{32}) \rho_{23}, \\
\frac{\partial \rho_{21}}{\partial t} &= (i\Delta_p - \Gamma_{21}) \rho_{21} - i(\Omega_p + D_{21})(\rho_{22} - \rho_{11}) + \\
&\quad + i(\Omega_c + D_{32}^* \rho_{23}) \rho_{31}, \\
\frac{\partial \rho_{31}}{\partial t} &= (i\Delta_p + i\Delta_c - \Gamma_{31}) \rho_{31} + i(\Omega_c + D_{32} \rho_{32}) \rho_{21} - \\
&\quad - i(\Omega_p + D_{21} \rho_{21}) \rho_{32}, \\
\frac{\partial \rho_{32}}{\partial t} &= (i\Delta_c - \Gamma_{32}) \rho_{32} - i(\Omega_c + D_{32})(\rho_{33} - \rho_{22}) - \\
&\quad - i(\Omega_p + D_{21}^* \rho_{12}) \rho_{31},
\end{aligned} \tag{5}$$

where $\Delta_p = \omega_p - \omega_{21}$, $\Delta_c = \omega_c - \omega_{32}$, and $\Gamma_{ij} = (\Gamma_i + \Gamma_j)/2$. Here, $\Gamma_2 = \Gamma_0 Z^2(\omega_{21})$ and $\Gamma_3 = \Gamma_0 Z^2(\omega_{32})$ are the spontaneous decay rates for the excited states $|2\rangle$ and $|3\rangle$, and Γ_0 is the decay rate for excitons in the absence of a photonic crystal. The function $Z(\omega_k)$ is called the form factor of the photonic crystal and is given in [29]. Next, by using the transform matrix method [30], we find the reflection and transmission coefficients

$$r(\omega_p) = \frac{-(i/2)(1/\sqrt{\varepsilon} - \sqrt{\varepsilon}) \sin(kd)}{\cos(kd) - (i/2)(1/\sqrt{\varepsilon} + \sqrt{\varepsilon}) \sin(kd)}, \tag{6a}$$

$$t(\omega_p) = \frac{1}{\cos(kd) - (i/2)(1/\sqrt{\varepsilon} + \sqrt{\varepsilon}) \sin(kd)}, \tag{6b}$$

where $n(\omega) = \sqrt{\varepsilon(\omega)}$ is the refractive index of the slab with the dielectric function $\varepsilon(\omega)$. The slab to be con-

sidered here is composed of a constant dielectric material doped with acceptor and donor QDs embedded in a photonic crystal. Therefore, the dielectric function $\varepsilon(\omega)$ can be separated into two parts and written as

$$\varepsilon(\omega_p) = \varepsilon_b + \chi(\omega_p), \tag{7}$$

where $\varepsilon_b = 4$ is the background dielectric constant and $\chi(\omega_p)$ is the susceptibility produced by the doped materials. The susceptibility of the medium can be calculated by solving set of equations (5) in steady-state regime, and is given by

$$\chi(\omega_p) = \frac{N_0 |\mu_{12}|^2}{\varepsilon_0 \hbar \Omega_p} \rho_{21}. \tag{8}$$

3. RESULTS AND DISCUSSION

In this section, we present some numerical results for the transmission, reflection, and absorption coefficients of incident light versus the probe field detuning under various conditions of the parametric region in Figs. 2–5. The physical parameters of the photonic crystal and their corresponding values can be found in [29]. The induced dipole moment of the QD is taken as $\mu_{12} = \mu_{23} = 0.4e \text{ nm}$ and its dielectric constant is $\varepsilon_Q = 6$. The vacuum decay rates for the QDs are taken as $\Gamma_2^0 = \Gamma_3^0 = 1 \mu\text{eV}$. The decay rates Γ_2 and Γ_3 are both calculated to be $3.5155 \mu\text{eV}$ in the absence of the Kerr effect [29]. The features of (a) transmission, (b) reflection, and (c) absorption of incident light versus the probe field detuning in the absence of DDI coupling parameters and for different values of the Rabi

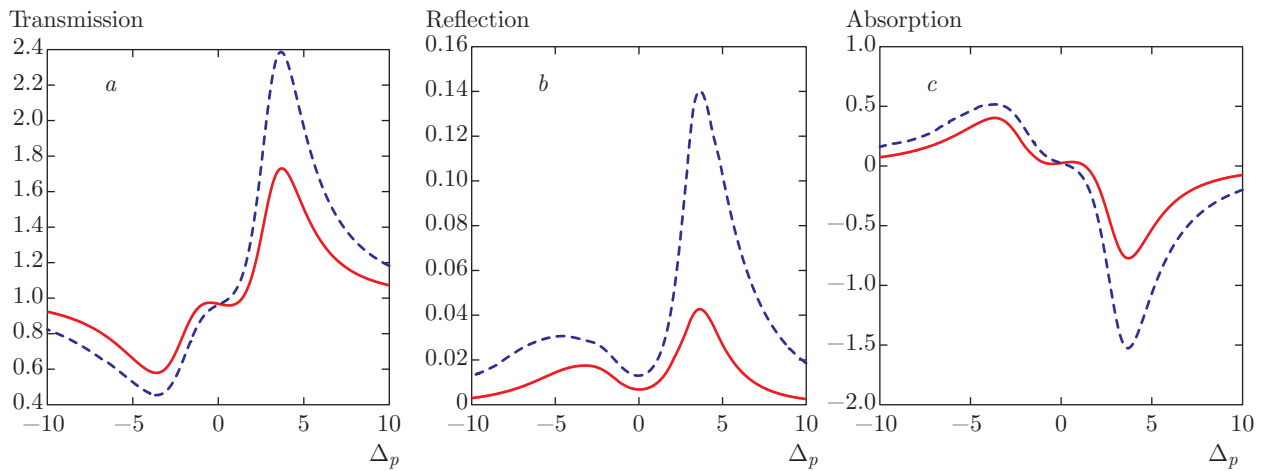


Fig. 3. (a) Transmission, (b) reflection, and (c) absorption properties of incident light versus the probe field detuning for different values of the DDI coupling parameter D_{21} . The solid lines correspond to $D_{21} = 1.2 \mu\text{eV}$ and the dashed lines to $D_{21} = 2.2 \mu\text{eV}$. The selected parameters are $m = 100$, $\Omega_c = 2.5$, $D_{32} = 0$, and $\Delta_c = 0$

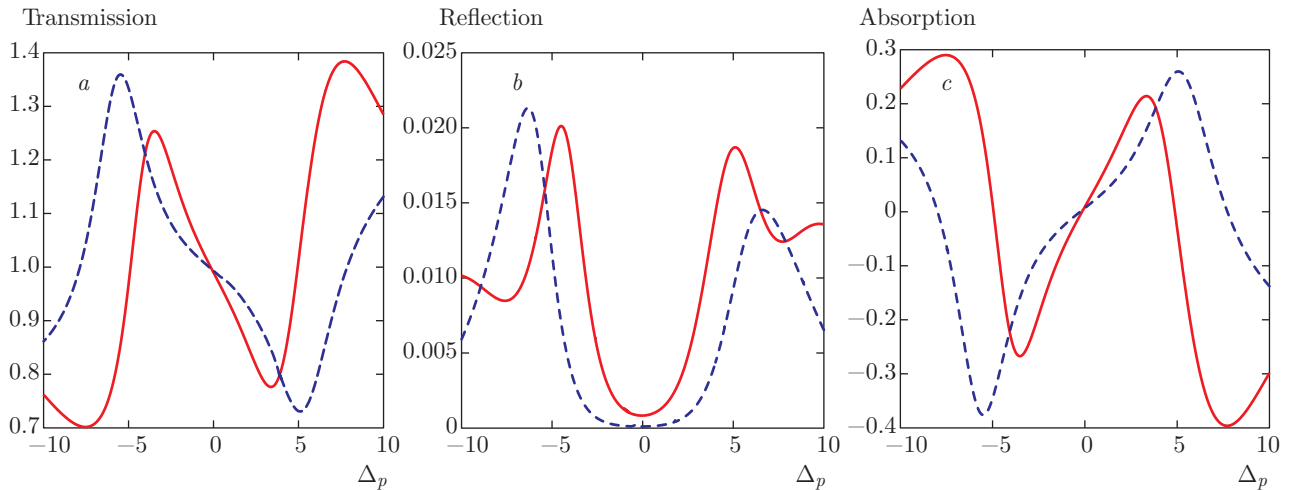


Fig. 4. (a) Transmission, (b) reflection, and (c) absorption properties of incident light versus the probe field detuning for different values of the DDI coupling parameter D_{32} . The solid lines correspond to $D_{32} = 5 \mu\text{eV}$ and the dashed lines to $D_{32} = 15 \mu\text{eV}$. The selected parameters are $m = 100$, $\Omega_c = 2.5$, $D_{21} = 1.2 \mu\text{eV}$, and $\Delta_c = 0$

frequency are presented in Fig. 2. The solid, dashed, and dotted lines respectively correspond to $\Omega_c = 2.5, 5,$ and 7.5 . We can see that by increasing the Rabi frequency of the applied field, the transmission of probe light can be enhanced and reaches its maximum value for $\Omega_c = 7.5$. However, the reflection and absorption coefficients of probe light reduce and reach their minimum value for $\Omega_c = 7.5$. We note that a peak in the curve of the reflectivity or transmittivity corresponds to subluminal pulse reflection or transmission. However, a dip corresponds to superluminal pulse reflection or transmission. Therefore, the group velocity of transmitted (reflected) light can be switched from su-

perluminal (subluminal) to subluminal (superluminal) by increasing the Rabi frequency of the coupling field. In other words, when we set $\Omega_c = 2.5$, the superluminal light is transmitted from the slab and subluminal light is reflected, while when we set $\Omega_c = 7.5$, the subluminal light is transmitted from the slab and superluminal light is reflected from it. Therefore, the switching from subluminal to superluminal or vice versa in transmitted and reflected pulses can be effected by adjusting the Rabi frequency of the applied field.

In the next step, we study the effect of the DDI coupling parameter D_{21} on the transmission, reflection, and absorption properties of the probe light. We can

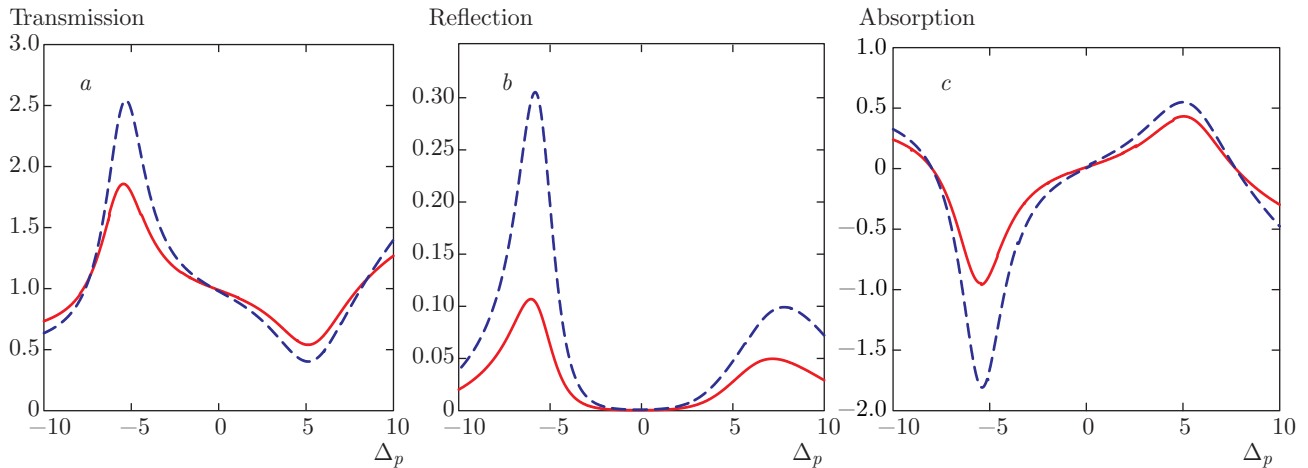


Fig. 5. (a) Transmission, (b) reflection, and (c) absorption properties of incident light versus the probe field detuning for different optical thickness values. The solid lines correspond to $m = 200$ and the dashed lines to $m = 300$. The selected parameters are $\Omega_c = 2.5$, $D_{32} = 5 \mu\text{eV}$, $D_{21} = 1.2 \mu\text{eV}$, and $\Delta_c = 0$

see that in the presence of the DDI coupling parameter D_{21} , the transmission coefficient in $\Delta_p \approx 5$ is greater than 1. In this region, the transmitted pulse has a peak, which corresponds to subluminal light propagation. By increasing the DDI coupling parameter, the transmission coefficient increases and reaches its maximum value equal to 2.4. From the reflection coefficient of the incident pulse, we can see that in the presence of the DDI coupling parameter D_{21} , the reflected pulse also has a peak, which corresponds to subluminal light propagation. Therefore, by considering the DDI coupling parameter D_{21} we conclude that subluminal phenomena occur simultaneously in both transmission and reflection pulses. In a conventional gas system, we can provide only subluminal or superluminal light propagation. But in a slab system, we achieve subluminal pulse reflection and subluminal light transmission simultaneously. The absorption properties of weak probe light versus the probe field detuning is displayed in Fig. 3c. It can be easily seen that the negative value of probe absorption can be obtained at $\Delta_p \approx 5$. As is known, negative absorption corresponds to probe amplification. Therefore, we can say that the probe field is amplified during its propagation through the medium. Accordingly, the probe field transmission increases (Fig. 3a). In Fig. 4, we display the (a) transmission, (b) reflection, and (c) absorption features of incident light versus the probe field detuning for different values of the DDI coupling parameter D_{32} . It can be seen that when we consider the effect of the DDI coupling parameter D_{32} , the peak in the transmission curve converts to the dip at $\Delta_p \approx 5$, and the dip at $\Delta_p \approx -5$ converts to the transmission peak. In this case, the value of the trans-

mission peak increases and is greater than unity. We conclude that switching from superluminal to subluminal light propagation or vice versa can be obtained by considering the DDI coupling parameter D_{32} . Observations on reflection properties of incident light show that the peak appears in the corresponding curve at $\Delta_p \approx -5$. Therefore, simultaneous peaks appear in the transmission and reflection curves of incident light. In this case, subluminal light propagation is obtained for both transmitted and reflected pulses. The absorption properties of incident light show that the probe amplification is obtained at $\Delta_p \approx -5$ when we consider the DDI coupling parameter. We finally discuss the optical thickness effect of a slab on the (a) transmission, (b) reflection, and (c) absorption properties of incident light. From Eqs. (6a) and (6b), it is found that the reflection and transmission coefficients depend on the thickness and the refractive index of the slab. For the resonance condition, the thickness of the slab is used in the form $d = 4\sqrt{\epsilon_b} \lambda_0 / 2m$, whereas for the off-resonance condition, it is taken as $d = 4\sqrt{\epsilon_b} \lambda_0 / (2m + 1)$, where m is an integer number. It can be realized that the transmission, reflection, and absorption coefficients change when we modify the parameter m .

4. CONCLUSION

We discussed the transmission, reflection, and absorption properties of incident light on a defect slab doped with acceptor and donor QDs embedded in a nonlinear photonic crystal. It is found that the dipole-dipole interaction between acceptor and donor QDs

can be used as an important parameter for adjusting the transmission, reflection, and absorption coefficients. We found that the probe amplification can be obtained in the presence of the dipole–dipole interaction coupling parameter. Moreover, we realized that the subluminal light propagation can occur simultaneously in transmitted and reflected pulses when we consider the effect of dipole–dipole interaction in the system. Our proposed model may be useful for developing all-optical devices based on photonic crystals doped with nanoparticles in future quantum communication systems.

REFERENCES

1. Y. Wu, J. Saldana, and Y. Zhu, *Phys. Rev. A* **67**, 013811 (2003).
2. Y. Wu and X. Yang, *Phys. Rev. A* **71**, 053806 (2005).
3. X.-X. Yang, Z.-W. Li, and Y. Wu, *Phys. Lett. A* **340**, 320 (2005).
4. S. Liu, J. Li, R. Yu, and Y. Wu, *Phys. Rev. A* **87**, 042306 (2013).
5. H. Xiong, L. Si, X. Lv, X. Yang, and Y. Wu, *Sci. China Phys. Mech. Astron.* **58**(5), 050302 (2015).
6. Z. Wang, *Opt. Commun.* **282**, 4745 (2009).
7. Z. Wang, B. Yu, J. Zhu, Z. Cao, S. Zhen, X. Wu et al., *Ann. Phys.* **327**, 1132 (2012).
8. J.-H. Li, *Phys. Rev. B* **75**, 155329 (2007).
9. J. Li, R. Yu, X. Hao, A. Zheng, and X. Yang, *Opt. Commun.* **282**, 4384 (2009).
10. J. Li, R. Yu, L. Si, X. Lü, and X. Yang, *J. Phys. B: Atom. Mol. Opt. Phys.* **42**, 055509 (2009).
11. W.-X. Yang, A.-X. Chen, L.-G. Si, K. Jiang, X. Yang, and R.-K. Lee, *Phys. Rev. A* **81**, 023814 (2010).
12. W.-X. Yang, J.-M. Hou, Y. Lin, and R.-K. Lee, *Phys. Rev. A* **79**, 033825 (2009).
13. W.-X. Yang, S. Liu, Z. Zhu, and R.-K. Lee, *Opt. Lett.* **40**, 3133 (2015).
14. E. Paspalakis and P. Knight, *Phys. Rev. A* **66**, 015802 (2002).
15. A. Joshi, S. Hassan, and M. Xiao, *Phys. Rev. A* **72**, 055803 (2005).
16. S. Dutta and K. R. Dastidar, *J. Phys. B: Atom. Mol. Opt. Phys.* **40**, 4287 (2007).
17. S. Dutta and K. R. Dastidar, *Mol. Phys.* **110**, 431 (2012).
18. H. Sattari and M. Sahrai, *Opt. Commun.* **311**, 83 (2013).
19. W.-X. Yang, W.-H. Ma, L. Yang, G.-R. Zhang, and R.-K. Lee, *Opt. Commun.* **324**, 221 (2014).
20. L.-G. Wang, H. Chen, and S.-Y. Zhu, *Phys. Rev. E* **70**, 066602 (2004).
21. D. Jafari, M. Sahrai, H. Motavalli, and M. Mahmoudi, *Phys. Rev. A* **84**, 063811 (2011).
22. Ziauddin, Y.-L. Chuang, R.-K. Lee, and S. Qamar, *Laser Phys.* **26**, 015205 (2016).
23. M. R. Singh, *J. Mod. Opt.* **54**, 1739 (2007).
24. M. R. Singh, *Phys. Lett. A* **363**, 177 (2007).
25. M. R. Singh, *Phys. Rev. A* **79**, 013826 (2009).
26. M. R. Singh, D. G. Schindel, and A. Hatef, *Appl. Phys. Lett.* **99**, 181106 (2011).
27. J. D. Cox, M. R. Singh, G. Gumbs, M. A. Anton, and F. Carreno, *Phys. Rev. B* **86**, 125452 (2012).
28. Z. Wang, S. Zhen, and B. Yu, *Laser Phys. Lett.* **12**, 046004 (2015).
29. M. R. Singh, C. Racknor, and D. Schindel, *Appl. Phys. Lett.* **101**, 051115 (2012).
30. L.-G. Wang, H. Chen, and S.-Y. Zhu, *Phys. Rev. E* **70**, 066602 (2004).